Momentum and Position Resolution at the CKOV plane for the GlueX detector system

Joachim Kuhn , Curtis Meyer

Carnegie Mellon University
Department of Physics
5000 Forbes Ave.
Pittsburgh, PA 15213

19 October 2004

Abstract

We present results from a Monte-Carlo study of the resolution of the (x, y)-position and of the momentum at the z-position of the proposed Čerenkov detector (CKOV) for the GlueX detector system. The method with which the tracks are traced in the magnetic field of the detector to a given z-position (along the beam-axis) is described as well.

1 Introduction

Tracks for this study were generated by the simulation package `HDFast` from the four charged pions in the final state of the reaction

$$\begin{aligned}\gamma p \rightarrow\ & \eta_1 p \\ & \eta_1 \rightarrow a_1^- \pi^+ \\ & \quad a_1^- \rightarrow \rho^\circ \pi^- \\ & \quad\quad \rho^\circ \rightarrow \pi^+ \pi^-\end{aligned}$$

The data set was generated with the program `genr8` with a peripheral phase space distribution and isotropically distributed decay angles [1]. For accepted events the momentum and vertex position of each track were then used to trace the particle through the magnetic field of the detector to the desired z-position with the method described below. This was performed for both, the original (generated) and the smeared (after `HDFast`) tracks. The opening angle between the traced momenta was then considered as a measurment for the angular resolution at the face of the CKOV.

1.1 Tracing of paricles in the magnetic field

A particle with charge q and velocity $\mathbf{v}$ in a magnetic field $\mathbf{B}$ experiences a force $\mathbf{F}$

$$\mathbf{F} = q \cdot (\mathbf{v} \times \mathbf{B}). \tag{1}$$

If the magnetic field is along the z-axis, $\mathbf{B} \equiv (0, 0, B)$, we get

$$F = q \, \frac{p_t}{m} \, B, \tag{2}$$

where $p_t \equiv |(p_x, p_y, 0)| = \sqrt{p_x^2 + p_y^2}$ is the absolute value of the transverse momentum of the particle.

The particle then describes a circle of radius R in the (x, y)-plane, whereas the z-component of the momentum remains unchanged. The force from the circular motion is given by

$$F = m \, \frac{v^2}{R} = \frac{p_t^2}{mR}. \tag{3}$$

Combining Eqs. 2 and 3 the radius R of the circular motion is given by

$$\begin{aligned} \frac{p_t^2}{mR} &= q \, \frac{p_t}{m} \, B \\ \Rightarrow \; R &= \frac{p_t}{qB} \end{aligned} \tag{4}$$

The rotation frequency, ω, of the particle in the magnetic field is then

$$\begin{aligned} \omega &= \frac{v}{R} \\ &= v \frac{qB}{p_t} \\ &= \frac{qB}{E} \end{aligned} \tag{5}$$

where we have used Eq. 4 and $v = p_t/E$.

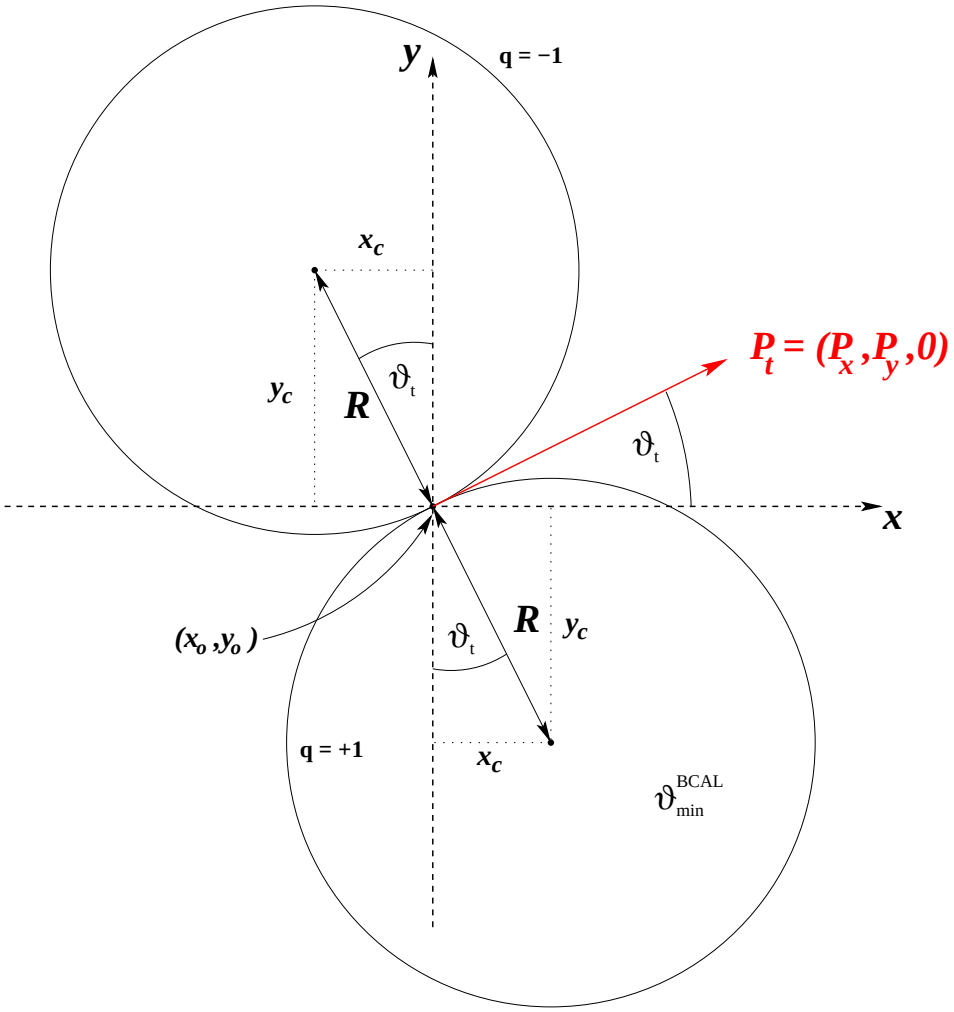

Fig. 1. Tracing of charged tracks in the (x, y) plane. The two circles represent the paths that positive and negative particles follow in a magnetic field in positive z-direction (out of the drawing plane).

1.2 Position tracing

The particle's trace in the (x, y)-plane describes a circle around the center position (x_c, y_c) with radius R (see Fig. 1). The center value of the circle is given by

$$\begin{aligned} x_c &= x_0 + qR\sin(\vartheta_t) \\ y_c &= y_0 - qR\cos(\vartheta_t), \end{aligned} \tag{6}$$

where (x_0, y_0) is the original vertex position, ϑ_t is the angle of $\mathbf{p}_t$ with respect to the x-axis, and q takes the values ± 1, depending on the charge of the

particle (see also Fig. 1). Then the position of the particle as a function of time t can be written as

$$\begin{aligned} x(t) &= x_c + R\cos(\omega t + \phi_t) \\ y(t) &= y_c + R\cos(\omega t + \phi_t), \end{aligned} \tag{7}$$

where we have defined $\phi_t \equiv \vartheta_t + q\frac{\pi}{2}$.

The z-position as a function of time is simply given by

$$\begin{aligned} z(t) &= z_0 + v_z t \\ &= z_0 + \frac{p_z}{E} t \end{aligned} \tag{8}$$

1.3 Momentum tracing

Since the B-field is along the z-direction, the absolute value of the momentum remains unchanged. To be more precise, the z-momentum p_z stays constant and the transverse momentum p_t is rotated along a circle with radius R, centered at (x_c, y_c) (see Fig. 1). The components of the momentum as a function of time can therefore be written as

$$\begin{aligned} p_x(t) &= p_t\cos(\omega t + \vartheta_t) \\ p_y(t) &= p_t\sin(\omega t + \vartheta_t) \\ p_z(t) &= p_z \equiv const. \end{aligned} \tag{9}$$

2 Position resolution at the face of the CKOV

Fig. 2 shows the track position in the (x, y)-plane after tracing the tracks to the z-position of the CKOV detector ($z = 420.0$ cm). The resolution as a function of $R = \sqrt{x^2 + y^2}$ is shown in Fig. 3(c), where we have plotted the difference between the traced position of the generated and the smeared track

$$\Delta R = R_{\text{gen}} - R_{\text{smear}} \tag{10}$$

Similar Fig. 4 and 5 show the resolution as a function of x- and y-position.

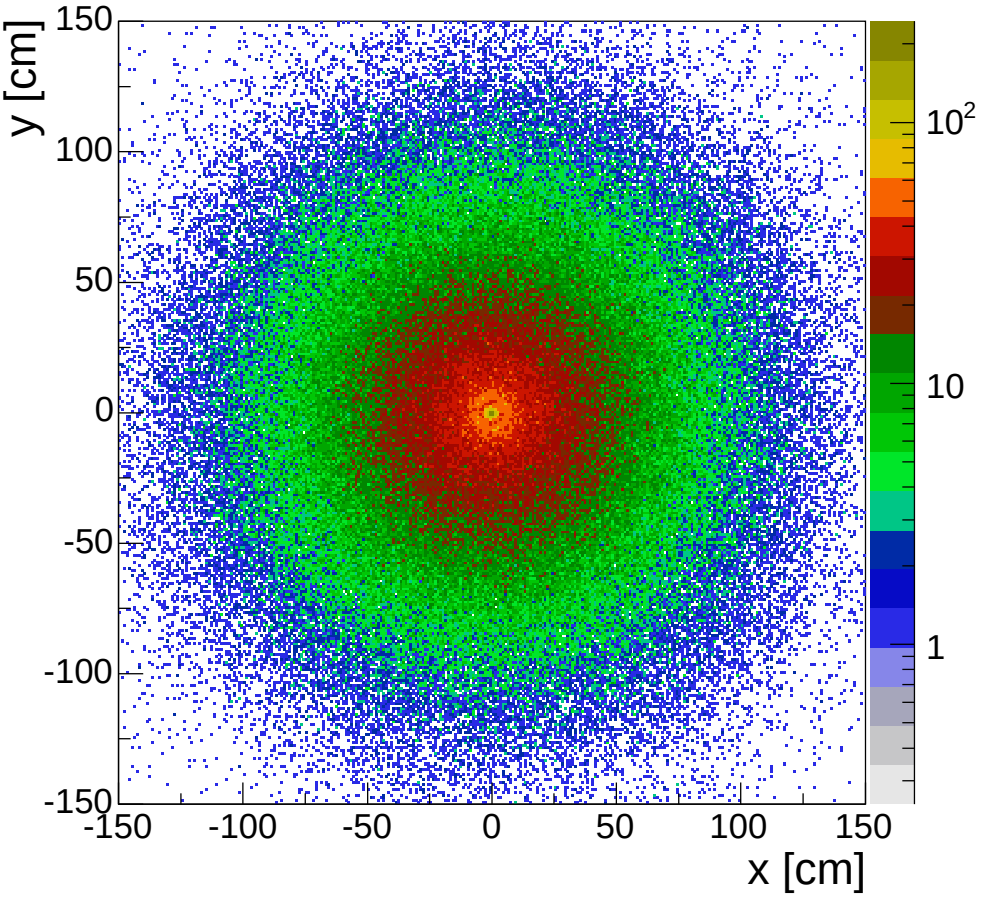

Fig. 2. y- vs x-position at $z = 420.0$ cm.

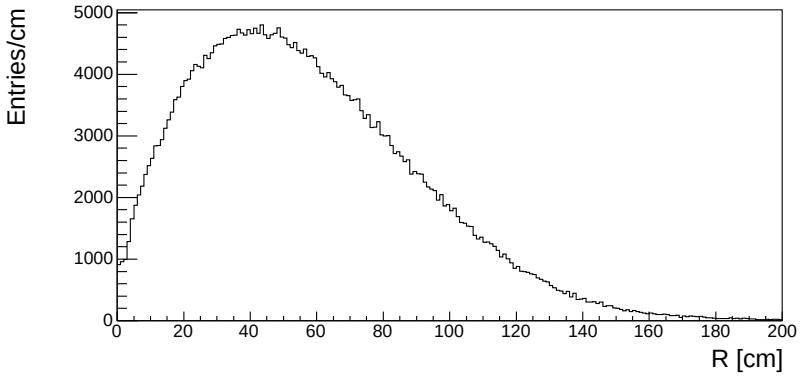

(a) unsmeared tracks

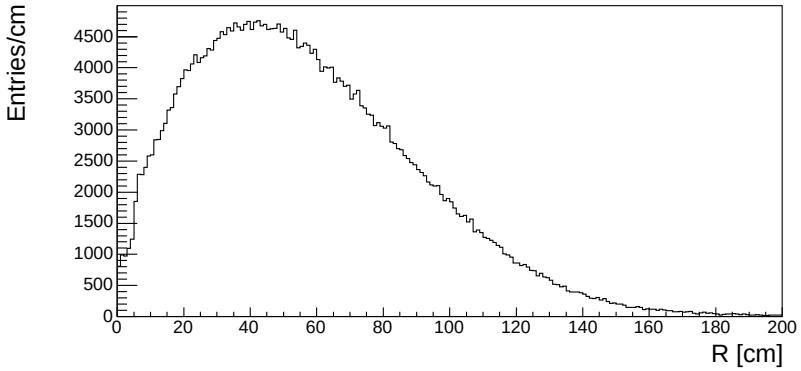

(b) smeared tracks

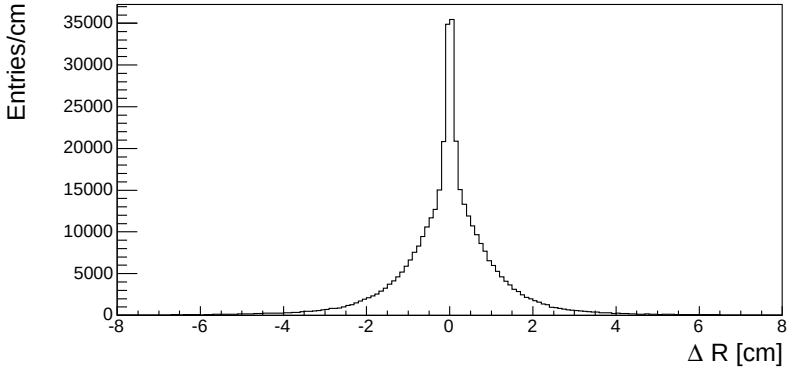

(c) ΔR

Fig. 3. Difference in position, R, for all four tracks at $z = 420$ cm.

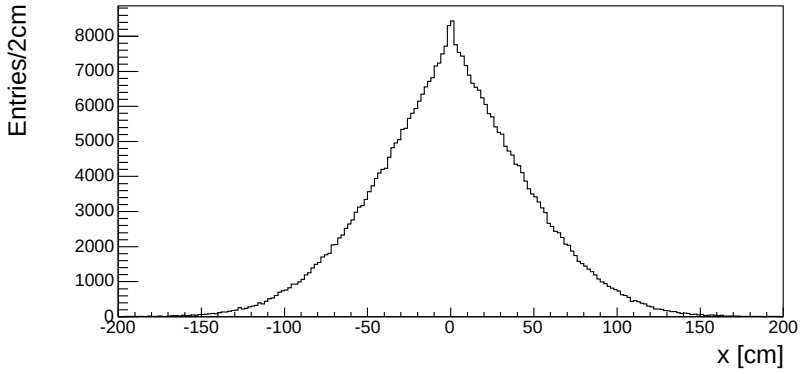

(a) unsmeared tracks

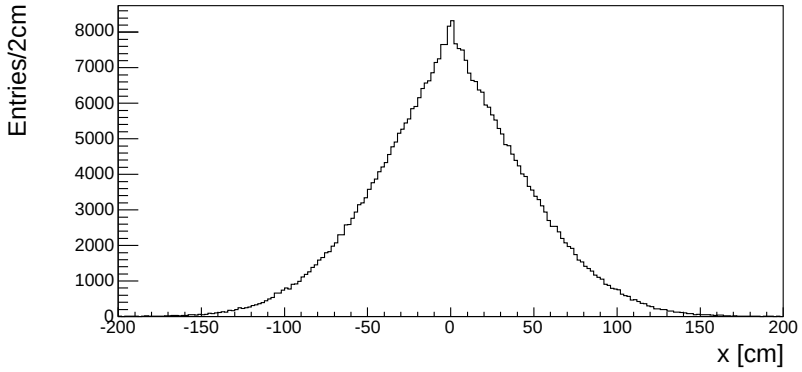

(b) smeared tracks

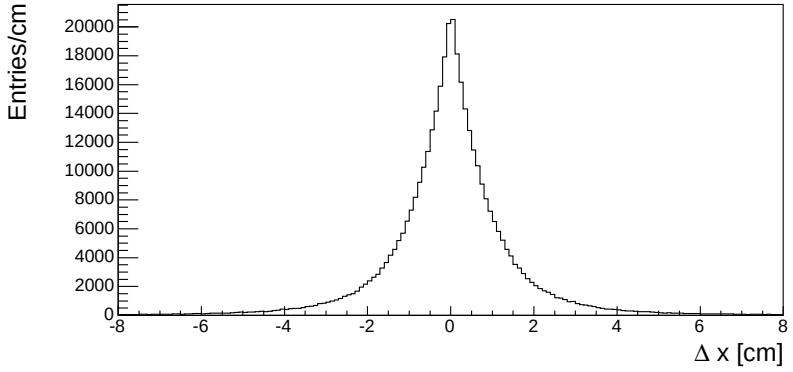

(c) ΔR

Fig. 4. Difference in position, x, for all four tracks at $z = 420$ cm.

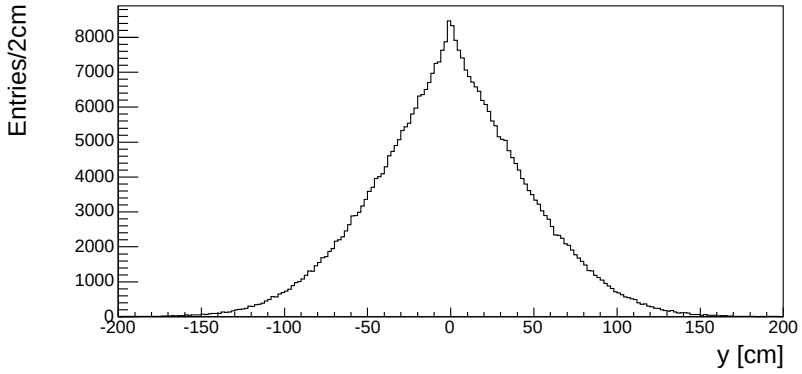

(a) unsmeared tracks

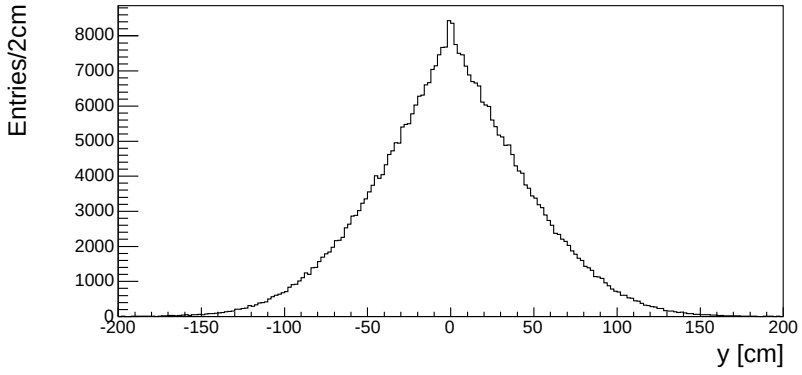

(b) smeared tracks

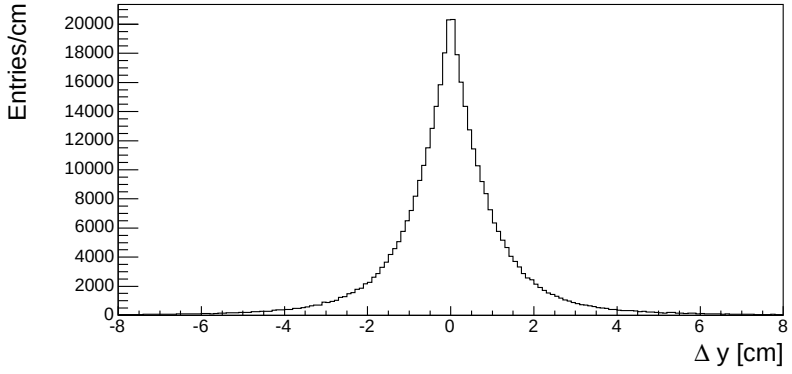

(c) ΔR

Fig. 5. Difference in position, y, for all four tracks at $z = 420$ cm.

3 Angular resolution of the momentum at the face of the CKOV

In order to determine the angular resolution, we compared the momenta of the generated vs the smeared track after tracing the tracks to the position of the CKOV. The opening angle $\Delta\theta$ between the two momenta was plotted for various ranges in track momentum, starting from 1.0 GeV/c up to 6.0 GeV/c in bins of 0.5 GeV/c. In Figs. 6, 8, and 10 these distributions are shown in increasing values of momentum from the top left to the bottom right. For each subset we determined the width of the $\Delta\theta$ distribution as the $\Delta\theta$ cutoff-value at which 63 %, 86 %, and 95 % of the events in the histogram were less than the cutoff value. In Figs. 6, 8, and 10 these cutoff-values are indicated by the red, black and blue vertical lines, respectively.

The angular resolutions (the width of the $\Delta\theta$ distributions) were then plotted against the value of the track momentum and are shown in Figs. 7, 9 , and 11. The results will be discussed in more detail in the following subsections.

3.1 Shifted target position

Events were generated with tracks originating from a vertex inside the target volume. In the "regular" detector geometry the target is centered at $z =$ 65 cm with a length of 15 cm and is located well upstream of the forward drift chambers (FDCs). Using events with their interaction vertices originating inside this volume would also inculde smearing (resolution) effects from the material between the target and the FDCs. We are interested in the angular resolution at the face of the CKOV, which is mostly determined by track momentum resolution in the drift chambers, independently of what material a particle has to pass through before reaching the FDCs. For this reason we created a fake target volume right in front of the FDCs in order to avoid having any material between the interaction vertex and the FDCs.

The distribution of the interaction vertex for this study was centered at $z =$ 217 cm, which is just after the downstream end of the central drift chamber (CDC) and in front of the most upstream FDC module. In order to avoid losing a lot of statistics because of the beam hole in the FDCs (which causes events that contain a forward track to be lost [1]), the target radius was inflated to $r = 20$ cm. At the same time the target length was constrained to a very small value ($L = 0.2$ cm).

The results using events from this data set are shown in Figs. 6 and 7 and display the expected behavior. Track angular resolution for 2 GeV/c and 5 GeV/c are approximately 1.75 mrad and 0.8 mrad, respectively. The exact values for all bins can be found in the appendix (Tabel A.1).

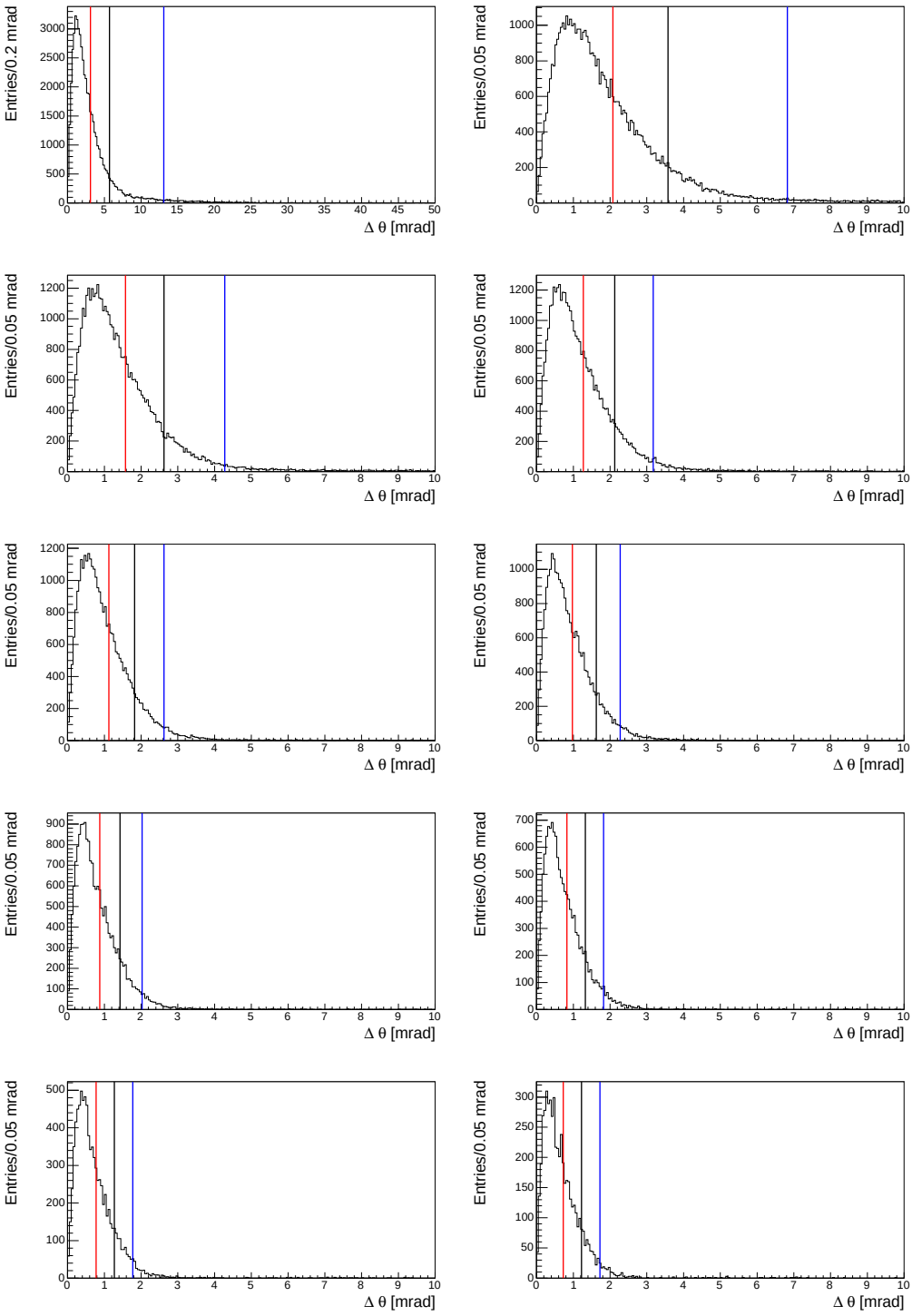

Fig. 6. $\Delta\theta$ distributions for track momenta p, from 1.0 GeV/c (top left) to 6.0 GeV/c (bottom right), using a shifted target (see text for details).

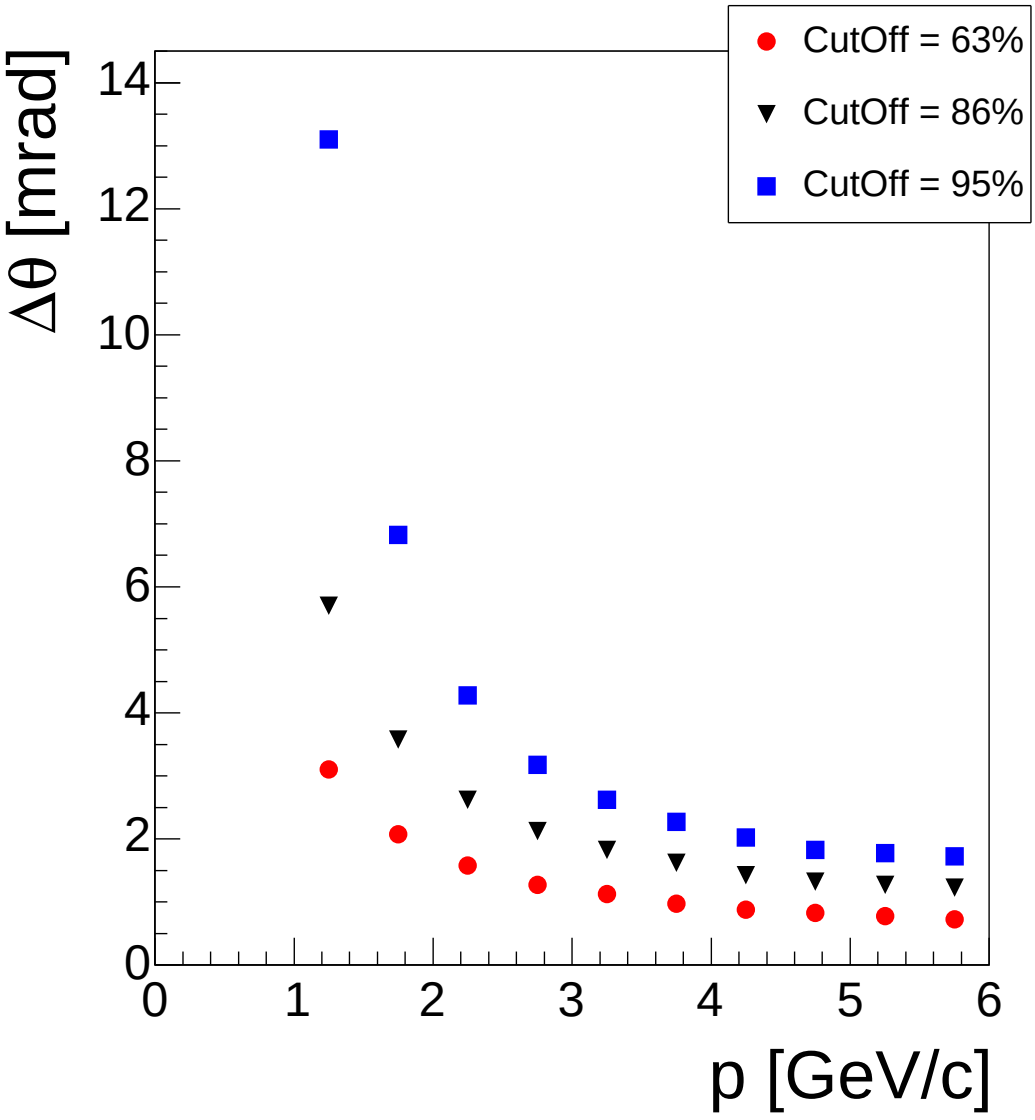

Fig. 7. Track angular resolution, $\Delta\theta$, as a function of track momentum p for tracks from events generated with a shifted target. For each 0.5 GeV/c momentum bin we determined the width of the $\Delta\theta$ distribution as the $\Delta\theta$ value at which 63 % (red circles), 86 % (black triangles), and 95 % (blue squares) of the events in the histogram were less than the cutoff value.

3.2 Shifted target position and shifted CKOV position

In a second study we used again the artificial target right in front of the most upstream FDC module. This time however the position of the CKOV was assumed to be further downstream ($z = 500$ cm) than in the "regular" geometry specifications. The results from these data are shown in Figs. 8 and 9 and show that there is not much difference as compared to the results in section 3.1 where the CKOV is at its nominal position of $z = 420$ cm. The slight increase in the resolution is likely due to the additional material between the two CKOV positions.

A table with all the values for the 10 momentum bins can again be found in the Appendix (Table A.2).

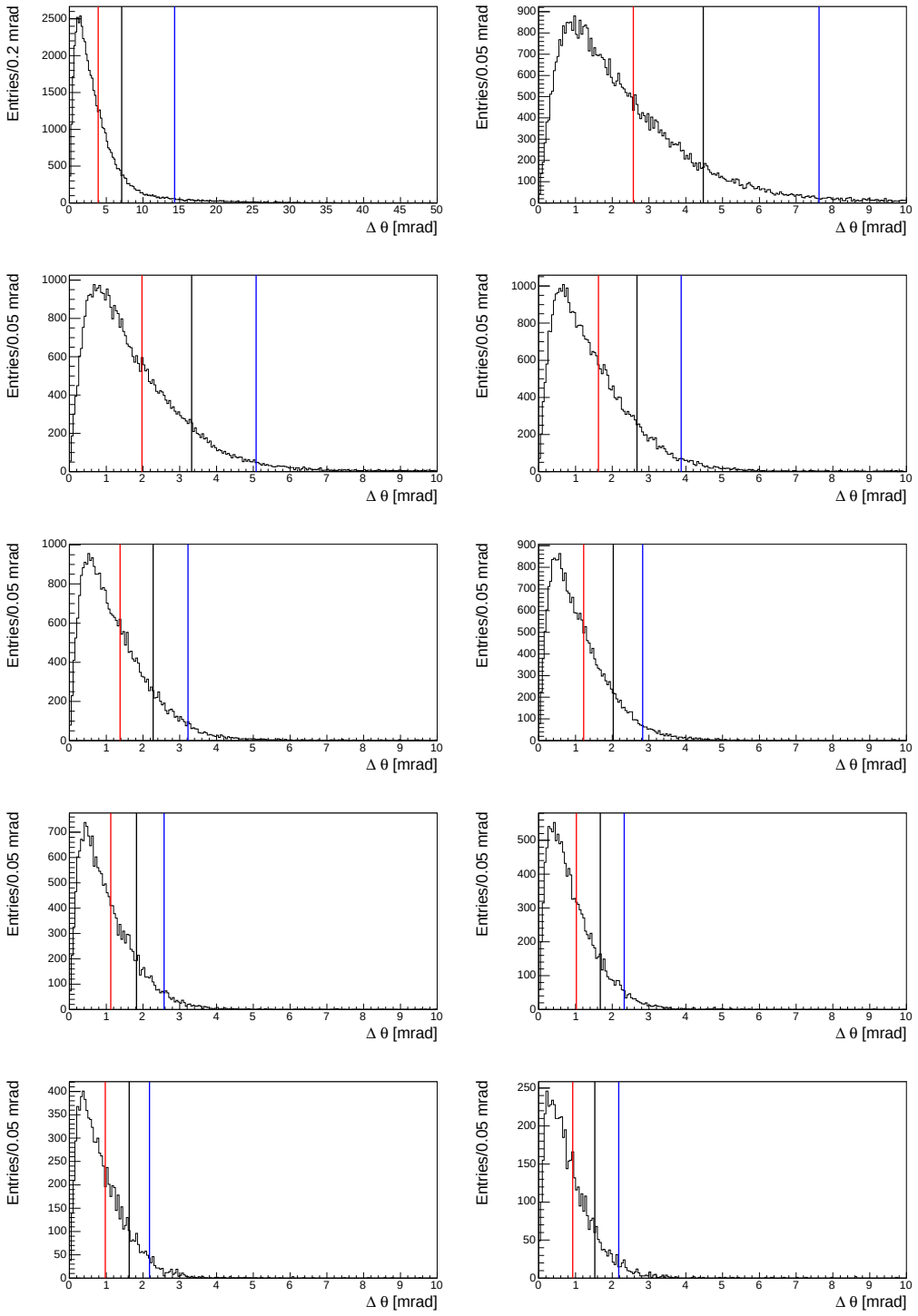

Fig. 8. $\Delta\theta$ distributions for track momenta p, from 1.0 GeV/c (top left) to 6.0 GeV/c (bottom right), using a shifted target and $z_{\mathrm{CKOV}} = 500$ cm (see text for details).

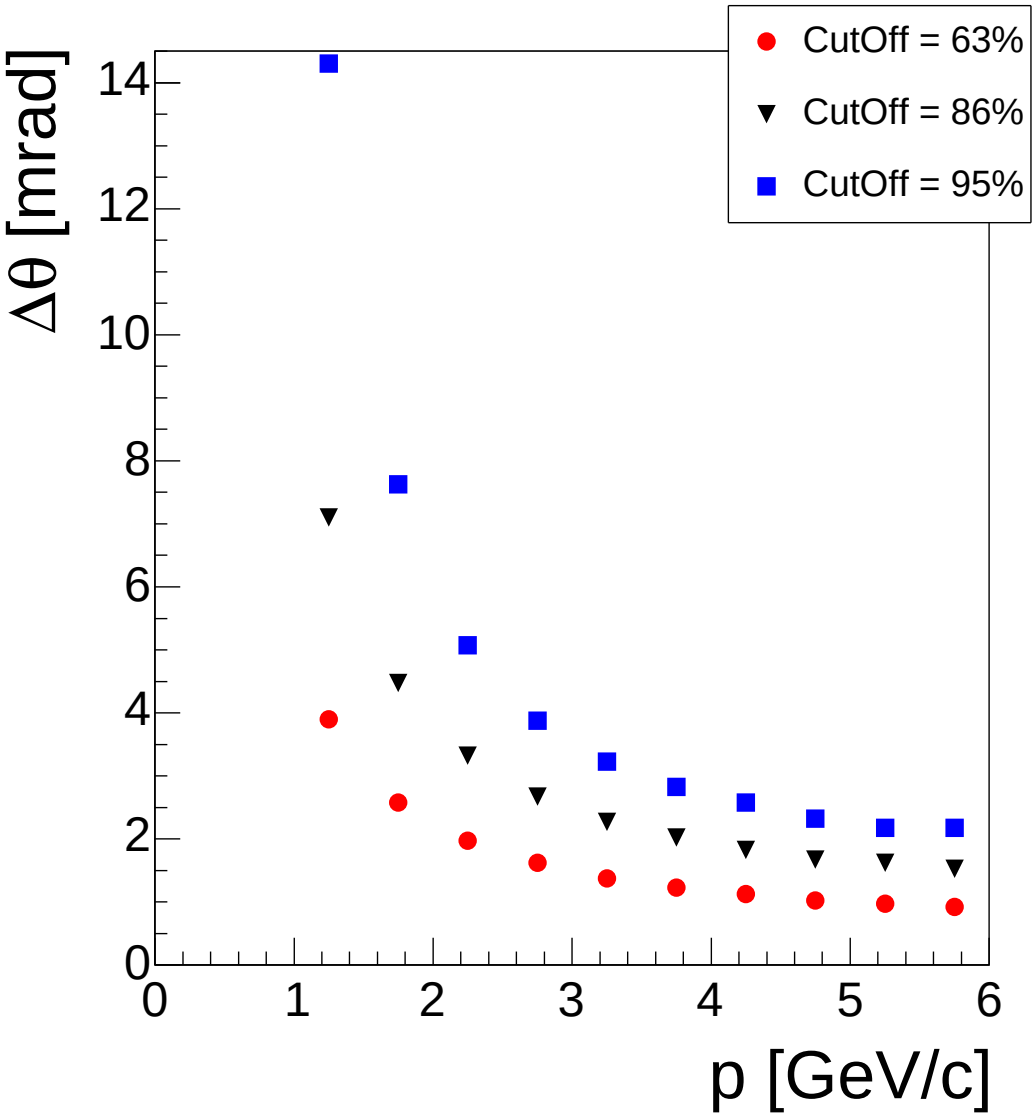

Fig. 9. Track angular resolution, $\Delta\theta$, as a function of track momentum p for tracks from events generated with a shifted target and $z_{\mathrm{CKOV}} = 500$ cm. For each 0.5 GeV/c momentum bin we determined the width of the $\Delta\theta$ distribution as the $\Delta\theta$ value at which 63 % (red circles), 86 % (black triangles), and 95 % (blue squares) of the events in the histogram were less than the cutoff value.

3.3 Regular target position

It is interesting to note what happens when one uses the "regular" detector geometry, where events are generated with tracks originating from a vertex inside the nominal target volume [1]. Fig. 11 shows that for tracks with momentum of 2 GeV/c and 5 GeV/c the angular resolutions deteriorate to approximately 5 mrad and 2 mrad, respectively. As already mentioned this is due to the additional material between the target and the FDCs, which should not be taken into account in our study.

Again, a table with all the values for the 10 momentum bins can be found in the Appendix (Table A.3).

[1] In the regular geometry the target is centered at $z = 65$ cm and has a length of $L = 15$ cm.

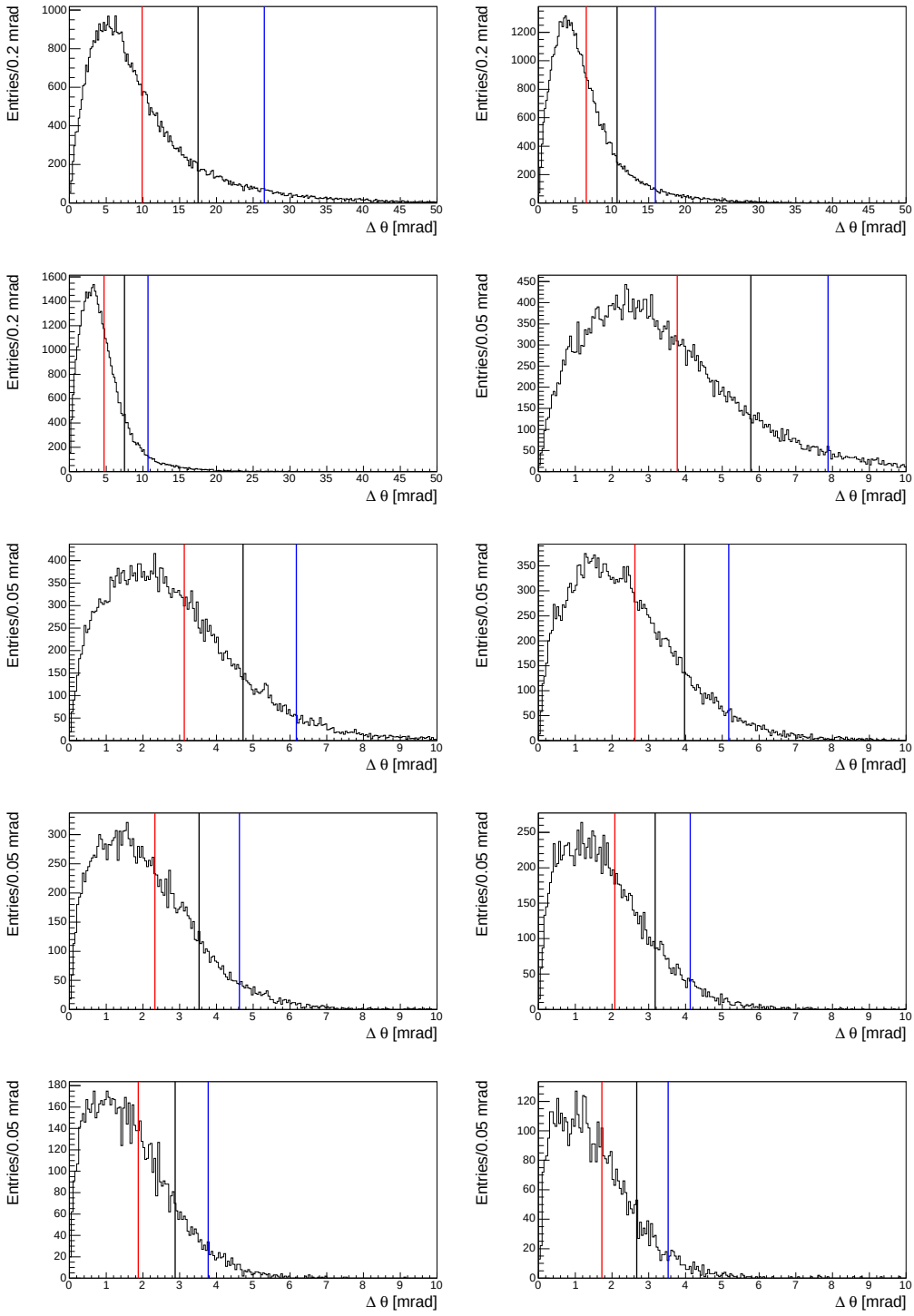

Fig. 10. $\Delta\theta$ distributions for track momenta p, from 1.0 GeV/c (top left) to 6.0 GeV/c (bottom right), using "regular" detector geometry (see text for details).

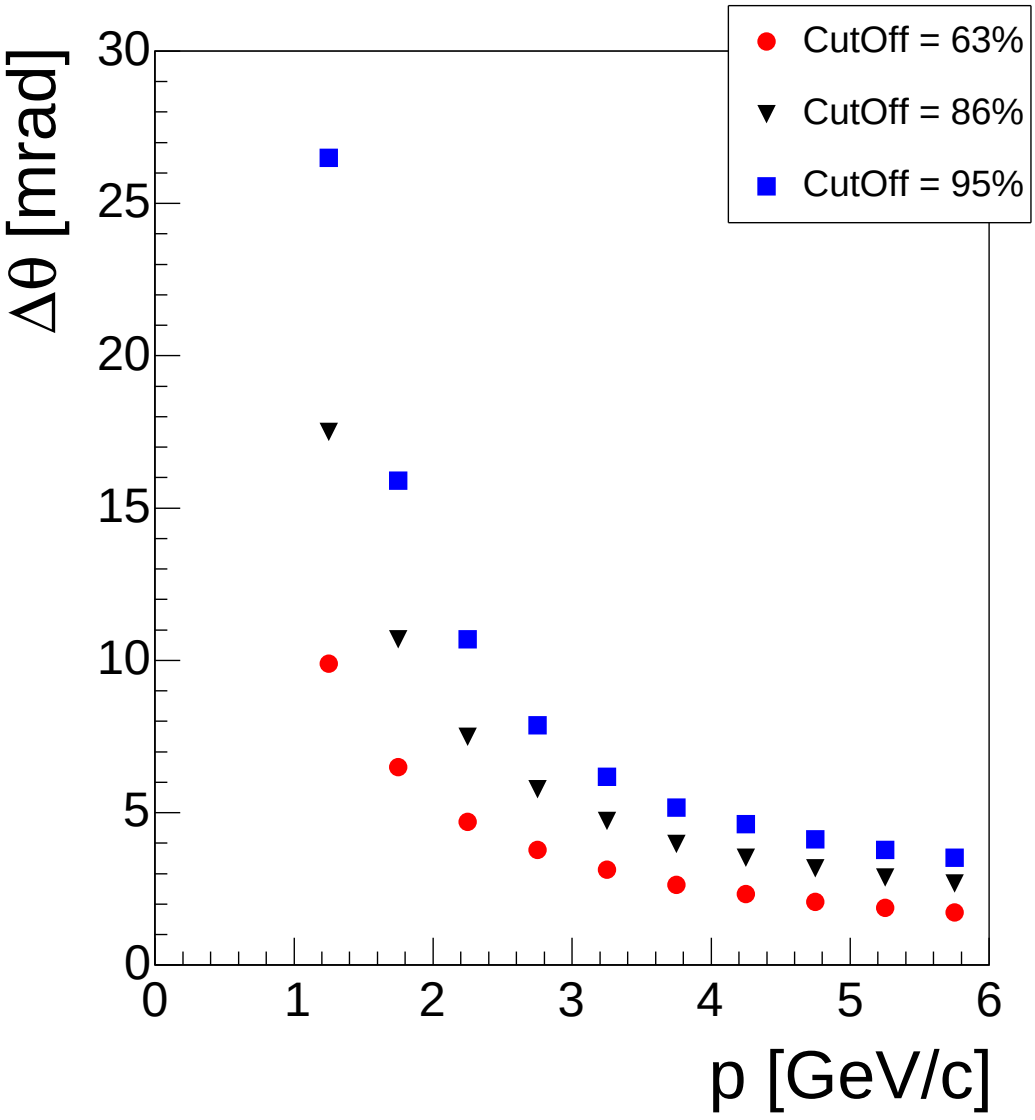

Fig. 11. Track angular resolution, $\Delta\theta$, as a function of track momentum p for tracks from events generated with the "regular" detector geometry. For each 0.5 GeV/c momentum bin we determined the width of the $\Delta\theta$ distribution as the $\Delta\theta$ value at which 63 % (red circles), 86 % (black triangles), and 95 % (blue squares) of the events in the histogram were less than the cutoff value.

Appendix

A Tables with the angular resolution results

A.1 Shifted target position

p [GeV/c]	63 %	86 %	95 %
	$\Delta\theta$ *for Cutoff* [mrad]		
1.0 – 1.5	3.1	5.7	13.1
1.5 – 2.0	2.075	3.575	6.825
2.0 – 2.5	1.575	2.625	4.275
2.5 – 3.0	1.275	2.125	3.175
3.0 – 3.5	1.125	1.825	2.625
3.5 – 4.0	0.975	1.625	2.275
4.0 – 4.5	0.875	1.425	2.025
4.5 – 5.0	0.825	1.325	1.825
5.0 – 5.5	0.775	1.275	1.775
5.5 – 6.0	0.725	1.225	1.725

Table A.1
Angular resolution as a function of track momentum p, using a shifted target.

A.2 Shifted target position and shifted CKOV position

p [GeV/c]	63 %	86 %	95 %
	$\Delta\theta$ *for Cutoff* [mrad]		
1.0 – 1.5	3.9	7.1	14.3
1.5 – 2.0	2.575	4.475	7.625
2.0 – 2.5	1.975	3.325	5.075
2.5 – 3.0	1.625	2.675	3.875
3.0 – 3.5	1.375	2.275	3.225
3.5 – 4.0	1.225	2.025	2.825
4.0 – 4.5	1.125	1.825	2.575
4.5 – 5.0	1.025	1.675	2.325
5.0 – 5.5	0.975	1.625	2.175
5.5 – 6.0	0.925	1.525	2.175

Table A.2
Angular resolution as a function of track momentum p, using a shifted target and $z_{\mathrm{CKOV}} = 500$ cm.

A.3 Regular target position

p [GeV/c]	63 %	86 %	95 %
	$\Delta\theta$ *for Cutoff* [mrad]		
1.0 – 1.5	9.9	17.5	26.5
1.5 – 2.0	6.5	10.7	15.9
2.0 – 2.5	4.7	7.5	10.7
2.5 – 3.0	3.775	5.775	7.875
3.0 – 3.5	3.125	4.725	6.175
3.5 – 4.0	2.625	3.975	5.175
4.0 – 4.5	2.325	3.525	4.625
4.5 – 5.0	2.075	3.175	4.125
5.0 – 5.5	1.875	2.875	3.775
5.5 – 6.0	1.725	2.675	3.525

Table A.3
Angular resolution as a function of track momentum p, using "regular" detector geometry.

References

[1] J. Kuhn, C. A. Meyer, Acceptance study for the gluex detector, gluex-doc-264, Carnegie Mellon University (2004).